

Magnetic interactions during sympathetic solar eruptions *

Yun-Chun Jiang¹, Yi Bi¹, Jia-Yan Yang¹, Rui-Sheng Zheng¹ and Jing-Xiu Wang²

¹ National Astronomical Observatories/Yunnan Observatory, Chinese Academy of Sciences, Kunming 650011, China; jyc@ynao.ac.cn

² National Astronomical Observatories, Chinese Academy of Sciences, Beijing 100012, China

Received 2008 June 16; accepted 2008 September 10

Abstract We present the first evidence for occurrences of magnetic interactions between a jet, a filament and coronal loops during a complex event, in which two flares sequentially occurred at different positions of the same active region and were closely associated with two successive coronal mass ejections (CMEs), respectively. The coronal loops were located outside but nearby the filament channel before the flares. The jet, originating from the first flare during its rise phase, not only hit the filament body but also met one of the ends of the loops. The filament then underwent an inclined eruption followed by the second flare and met the same loop end once more. Both the jet and the filament eruption were accompanied by the development of loop disturbances and the appearances of brightenings around the meeting site. In particular, the erupting filament showed clear manifestations of interactions with the loops. After a short holdup, only its portion passed through this site, while the other portion remained at the same place. Following the filament eruption and the loop disappearance, four dimmings were formed and located near their four ends. This is a situation that we define as “quadrupolar dimmings.” It appears that the two flares consisted of a sympathetic pair physically linked by the interaction between the jet and the filament, and their sympathy indicated that of the two CMEs. Moreover, it is very likely that the two sympathetic CMEs were simultaneously associated with the disappearing loops and the quadrupole dimmings.

Key words: Sun: activity — Sun: coronal mass ejections (CMEs) — Sun: filaments — Sun: flares — Sun: magnetic fields — Sun: corona

1 INTRODUCTION

Sympathetic solar eruptions, including flares and coronal mass ejections (CMEs), are consecutive eruptions that occur almost simultaneously in different active regions (AR) having a certain physical connection. The existence of sympathetic flares was evidenced by some statistical studies (Pearce & Harrison 1990; Moon et al. 2002; Wheatland & Craig 2006) and a few observational studies of individual sympathetic flares (Shi et al. 1997; Gopalswamy et al. 1999; Zhang et al. 2000; Wang et al. 2001). However, some recent observations showed that successive flarings can also occur in different positions along a magnetic polarity inversion line (PIL) of the same AR. Goff et al. (2007) reported that flare ribbons of a series of flares not only separate but also shift along the PIL as magnetic reconnection progresses stepwise to neighboring flux tubes. Wang et al. (2007) also suggested that the destabilization of a flux loop system by heating from the extended ribbon of an initial flare led to filament eruption with a successive

* Supported by the National Natural Science Foundation of China.

flaring. On the other hand, sympathetic CMEs were very rare phenomena and only a few plausible sympathetic CME pairs were reported on the basis of observations with a white-light coronagraph (Simnett & Hudson 1997; Moon et al. 2003). As indicated by Cheng et al. (2005), it is noteworthy that sympathetic CMEs can originate from different filament eruptions in the same AR. It is clear that the key to the sympathy of eruption events is the physical connection between them. When different driving agents linking sympathetic flares have been found, the possible driving mechanism of sympathetic CMEs remains unclear, and it is also unclear how or whether sympathetic flares can relate to sympathetic CMEs. In order to identify the sympathy of successive CMEs, a direct and creditable way is to investigate the possible magnetic interactions between their corresponding on-disk source regions.

A strongly related question is whether the ubiquitous coronal loops in the solar atmosphere (Aschwanden 2004) can play an important role in interaction or reconnection of two erupting magnetic structures. Khan & Hudson (2000) presented direct evidence that disappearances of transequatorial interconnecting loops can be sources of certain CMEs, and suggested that flare-induced shock waves could destabilize these loops. Different from the so-called bipolar double dimmings (BDDs) that explain the evacuated feet of a large-scale flux rope ejection in some CME events (Sterling & Hudson 1997; Jiang et al. 2006a, 2007c), remote brightenings and dimmings that were far from the CME source region have been suggested to be caused by the interaction of expanding twisted flare loops with overlying large-scale loops (Manoharan et al. 1996; Liu et al. 2006; Jiang et al. 2006b). However, such interaction was not directly observed until now since the putatively overlying loops themselves were invisible probably as a result of insufficient temperature and density. The direct observation of the interaction between an erupting structure and coronal loops may well shed light on not only the trigger mechanism of loop eruptions but also the developments of associated dimmings and CMEs.

More recently, Jiang et al. (2007d) found that an erupting filament can interact with a coronal hole, and in particular, Jiang et al. (2008) showed that a sole flare can not only trigger a CME but also simultaneously trigger an eruption of interconnecting loops through interactions with a transequatorial jet, which can lead to two sympathetic CMEs. On 2003 November 18, a jet from an initial flare impacted a filament and some coronal loops, and then the filament obliquely erupted and impacted the loops again. This led to the second flare, the loop disappearances and the formation of four dimmings. In this paper, we present clear evidence for occurrences of magnetic interactions between the jet, the filament and the coronal loops during this rare and complex event. We further show that both the sympathetic flare and CME pairs were physically connected by the jet/filament interaction, and that the four dimmings were due to the filament eruption and the loop disappearances.

2 OBSERVATIONS

The observations used in the present study include:

1. Full-disk $H\alpha$ images from Kanzelhöhe Solar Observatory (KSO) in Austria (Otruba & Pötzi 2003). We used $H\alpha -0.3 \text{ \AA}$ off-bands ($H\alpha$ center) images with a cadence of 1 (1)-minute and a pixel size of about $2.2''$ ($1''$), recorded by a $1k \times 1k$ 10 bit CCD (a $2k \times 2k$ Apogee 14 bit KX4 camera). Since the KSO's observations started at 07:33 UT, we also examined full-disk $2k \times 2k$ $H\alpha$ center images from the Yunnan Astronomical Observatory (YNAO) in China.
2. 171 and 195 \AA images from the *Transition Region and Coronal Explorer* (TRACE; Handy et al. 1999) with a pixel size of $0.5''$ and varying cadence and wavelength. For the event, the TRACE observations have a data gap from 08:03 to 08:22 UT.
3. Full-disk EUV images with a pixel resolution of $2.6''$, full-disk line-of-sight magnetograms with a pixel size of $2''$ and a 1-minute cadence, and the C2 (C3) white-light coronagraph data that cover the range 2 (4) to 6 (32) solar radii, from the Extreme Ultraviolet Telescope (EIT; Delaboudinière et al. 1995), the Michelson Doppler Imager (MDI; Scherrer et al. 1995) and the Large Angle and Spectrometric Coronagraphs (LASCO; Brueckner et al. 1995) aboard the *Solar and Heliospheric Observatory* (SOHO), respectively. EIT 195 \AA images were obtained continuously with a 12-minute cadence while 171, 284 and 304 \AA images were taken only once every 6 hr. We also used the CME height-time data that are available at the LASCO Web site.

3 RESULTS

On 2003 November 18, two flares, “FL1” and “FL2,” successively occurred in AR 10501 (N03°, E18°). The FL1 (FL2) of X-ray class M3.2 (M3.9) had start, peak and end times at around 07:23 (08:12), 07:52 (08:31) and 08:06 (08:59) UT, respectively. Note that the time interval between the FL1 end and the FL2 start was only 6 minutes.

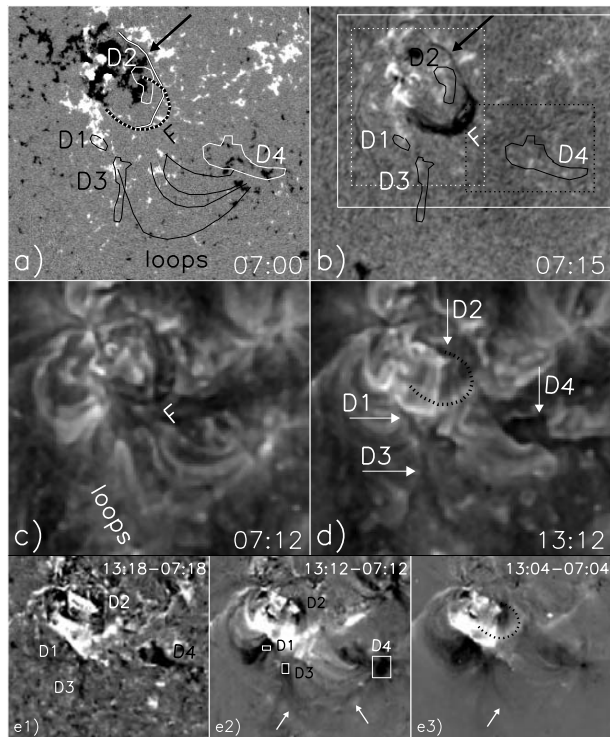


Fig. 1 (a) MDI magnetogram, (b) YNAO $H\alpha$ image, direct EIT 195 Å images (c) before and (d) after the flares, and 304, 195 and 284 Å fixed-base difference images (panels e1-e3, respectively). In (a), the outlines of the F in (b), the well-defined loops in (c), and the four dimmings determined from panel e1 are plotted. The F outlines are also plotted as black dashed curves in (d) and panel e3. The black dashed and white dashed (solid) boxes indicate the field-of-views (FOVs) in Fig. 3 and panels b1-b4 (panels c1-c4 and d1-d4) in Fig. 2. The FOV is $660'' \times 600''$. North is up and West is to the right.

Figures 1a and 1b show the general appearance of the AR in the MDI magnetogram and YNAO $H\alpha$ image before the flares, respectively. A fishhook-like filament lay on the PIL at the western boundary of the AR, and consisted of two twined sections: a southern thick loop-like one, “F”, and a northern thin one (indicated by black arrows). The former erupted during the FL1 and preceded the FL2, while the latter remained after the two flares. In direct EIT 195 Å images, several well-defined coronal loops to the south of the F can be visible before the flares (Fig. 1c) and their outlines plotted in Figure 1a indicate that their footpoints rooted in opposite-polarity plage regions outside the filament channel around the AR’s southern periphery. After the flares (Fig. 1d), however, these loops disappeared and four dimmings, “D1”, “D2”, “D3” and “D4”, were formed. The D4, the largest dimming, was quite obvious and close to the western footpoints of the loops, and the D1, D2 and D3, despite being smaller, can also be discerned. In panels e1-e3 of Figure 1, we compare the difference images obtained by subtracting pre-flare images at EIT 304, 195 and 284 Å. When loop-like dimmings appearing along the pre-flare loops indicating

the disappearance of these loops (indicated by the white arrows), the D1-D4 were clearly discernible and showed similar locations and shapes in these lines, probably suggesting that they were due to a loss in density rather than a decrease in temperature in the coronal plasma (Thompson et al. 1998). The D1-D4 boundaries (the F outline) determined from the 13:18 UT 304 Å (the 07:15 UT H α) image are also superposed in Figure 1. We see that the northern F end was near the D2 of negative-polarity but the D1 is located on positive-polarity regions around the southeastern F end. Thus, it appears that the D1-D2 is composed of BDDs in association with the F eruption. On the other hand, the D3 and D4 were around the opposite-polarity footpoint regions of the disappeared loops and very likely resulted from the loop eruptions (Jiang et al. 2008). In this event, the region around the D4 was a key site for the loop disappearances, so it is termed “D4R” throughout this paper for convenience.

Figure 2 shows the morphological evolutions of the event in EIT EUV, *TRACE* EUV, and YNAO and KSO H α observations. The FL1 occurred near the southeastern F end but did not result from any eruption of the F (see panels c1-c4). It consisted of two ribbons slightly expanding normal to the PIL but having no clear shift along the PIL (Miklenic et al. 2007). On the other hand, the FL2 was a result of the F eruption. It is clear that the F eruption occurred in the course of the FL1 and preceded the FL2 start (see panels c2-c5 and d1-d4). This result is consistent with Kahler et al. (1988) that filaments began to erupt before the starting times of associated flares. Although the eruption produced some H α brightenings in combination with the FL1 flare ribbons in the early eruption phase (see panel c5), the two ribbons of the FL2 were spatially separated from that of the FL1 and showed more obvious expansion normal to the PIL after the start time of the GOES FL2 (see panels c6-c8 and b3). As a striking characteristic of the event, the two flares were physically linked by a bright jet. The jet started to eject from the FL1 core at about 07:40 UT during the FL1’s rise phase, which can be simultaneously seen in EIT (see panels a3 and a4) and *TRACE* (see panel b2) 195 Å images. Similar to the cases shown by Švestka et al. (1990), Chae et al. (1999b) and Jiang et al. (2007a), the EUV jet had a bright chromospheric counterpart, i.e., a bright H α jet (see panels c3 and c4), possibly suggesting that it had significantly higher density or/and temperature than that of the F. It is clear that the jet from one F end nearly moved parallel to the F axis and directly hit the southeastern part of the F (see panels b2, c3 and c4) immediately after its first appearance, and then the F began to slowly erupt (see panel d1) accompanied by the formation of the D1 and D2 (see panel a4). Therefore, the F eruption was most likely due to the direct interaction occurring between the jet and F. The 07:55 UT H α center image (panel c4) clearly shows that the erupting F was hit and squeezed by the jet. When this eruption was obvious in the H α blue-wing, the dark F became ambiguous at the H α center (see panels c3 and c4), which might be associated with the ionizing and heating of the filament plasma. Considering that the FL2 is a result of the F eruption, as well as the closeness in time but difference in space of the FL1 and the FL2, the two flares consisted of a clear sympathetic pair physically connected by the jet. This is similar to successive flarings occurring in the same AR recently reported by Goff et al. (2007) and Wang et al. (2007). Although we cannot completely exclude the possibility that the initial flare destabilized neighboring flux tubes/loops and then led to successive flarings, we believe that the jet/F interaction in this case was the dominant driving mechanism of the F eruption since no obvious shift of the FL1 ribbons along the PIL was observed.

The jet and the F eruption were followed by a series of activities. First, the D1 and D2 were formed and very close to the two F ends at the F eruption start (see panels a4 and a5), implying that their formation was closely related to this eruption. The D2 then decreased in area while the D1 was separated from the southeastern F end due to the expansion of the FL2 ribbons (see panel a8). Secondly, the loops were clearly disturbed (see panels a3 and a4), and the D3 and D4 began to appear (indicated by the thin white arrows in panels a3-a5) around their two ends. Note that the D1, D2 and a portion of the D3 can be more clearly discernible in high-resolution *TRACE* direct and difference images (see panels b3 and b4). Finally, a clear H α brightening appeared near the D4R (see panels c3 and d1), which later can also be seen in EIT images (indicated by the thin black arrows in panel a5). It is noted that, despite no signal in the H α images, the jet traveled a long distance toward the loops and the D4R. This is clearly seen in the EIT images at 07:47 and 07:58 UT (indicated by the thick white arrows in panels a3 and a4). Therefore, it seems that a portion of the jet also threaded its way through the F body and then directly impacted the loops and the D4R. Similar to the case of jet/loop interaction recently reported by Jiang et

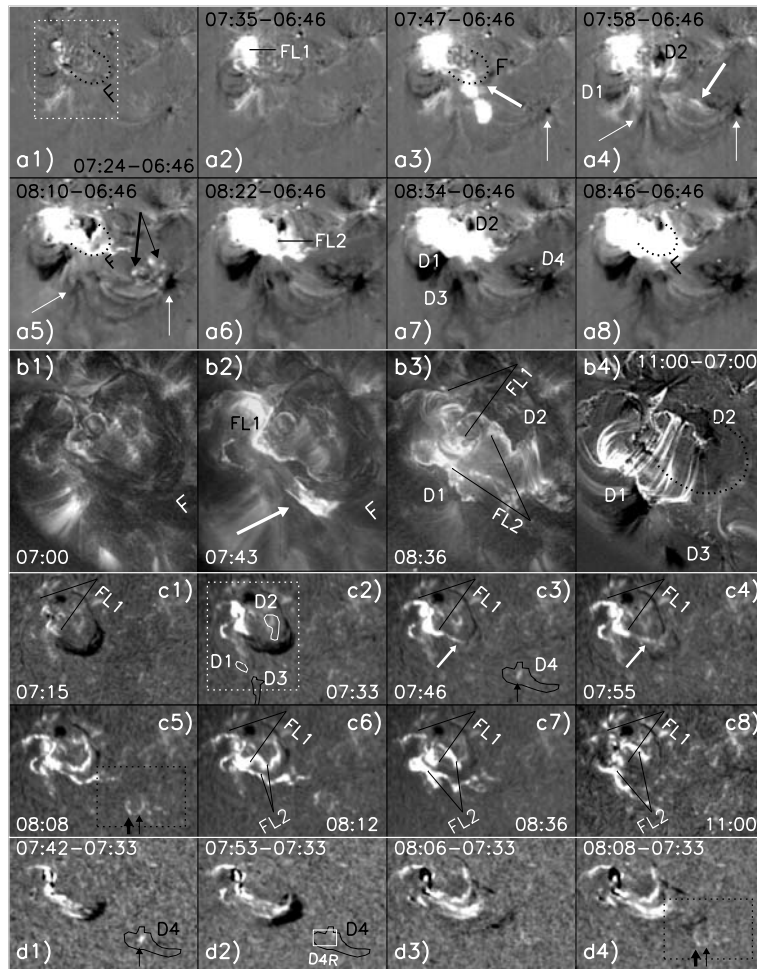


Fig. 2 EIT 195 Å fixed-base difference images (panels a1-a8) with a FOV as in Fig. 1. *TRACE* 171 Å (panel b1) and 195 Å (panels b2-b3) direct images, and 171 Å difference images (panel b4) with a FOV of $290'' \times 340''$. YNAO and KSO $H\alpha$ center (panels c1-c8) and blue-wing fixed-base difference (panels d1-d4) images with a FOV of $600'' \times 420''$. 'FL1' marks the extent of the first flare, and 'FL2' the two separating ribbons of the second flare. The thin (thick) white arrows indicate the D3 and D4 (the jet), and the thin (thick) black arrows indicate the brightenings due to the disturbance or hit from the jet (the erupting F). The outlines of the F and the D1-D4 as in Fig. 1 are also plotted. The white (black) dashed box indicates the FOV of panels b1-b4 (Fig. 3).

al. (2008), the loop's activities were possibly due to the jet impact, while the brightenings near the D4R were associated with not only such activities but also the following jet impact.

Afterwards, the F obliquely erupted towards the southwest direction (see panels d2-d4). Since the eruptive region was located in the eastern hemisphere, taking the projection effect into account, the erupting F was not normal to the solar surface but had an inclined eruption path (Jiang et al. 2007b,d), otherwise, it would erupt in the eastern direction. By about 08:08 UT, the F reached the D4R (see panel d4) and new, second $H\alpha$ and EUV brightenings were observed around this site (indicated by the thick black arrows in panels a5, c5 and d4). Then, the loop disturbances and the D1-D4 underwent further development and new dimmings extended to cover the new brightenings (see panels a6-a8). Therefore,

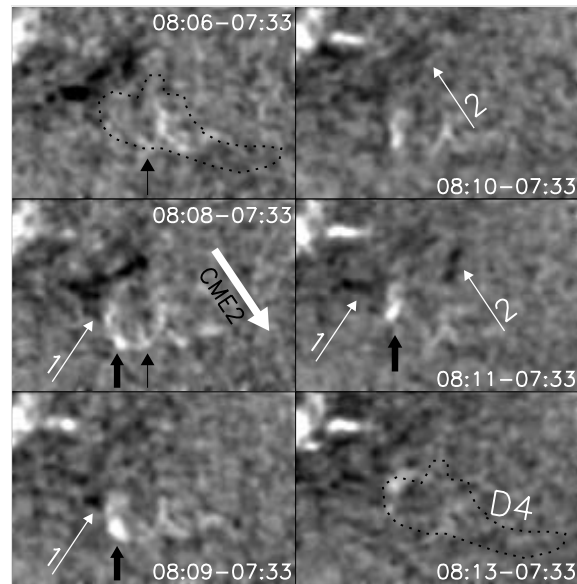


Fig. 3 KSO $H\alpha$ blue-wing fixed-base difference images. The thin (thick) black arrows indicate the first (second) brightenings. The thin white arrows, ‘1’, indicates the portions of the F that cannot pass the D4R, while, ‘2’ the portion that passed the D4R after a short stop. The thick white arrow indicates the eruption direction of the CME2. The outlines of the D4 as in Fig. 1 are also plotted. The FOV is $280'' \times 190''$.

as another distinct characteristic of the event, it seems that the F also interacted with loops in the D4R. This is strongly evidenced by the following F evolution, which is shown by the close-up view of the D4R in Figure 3. It is clear that the arch-like erupting F was blocked by the D4R, and so did not completely cross it. At 08:08 UT, when the F met the D4R, the second brightening was clearly seen. The F then broke into two parts, ‘1’ and ‘2’. The western part 2 continued erupting after a brief stay, but the eastern part 1 cannot pass the eastern D4R boundary and stopped here. By 08:12 UT, when the FL2 started, the F was no longer discernible. Such erupting behavior of the F, which has not been reported before, clearly indicated its direct interaction with the D4R. Since the D4R was close to the western footpoints of the disappearing loops, it is very likely that magnetic reconnection occurred between the fields of the F and the loops, which led to the released energy producing the brightenings. It is also noteworthy that, as seen in panel b4 of Figure 2, the post-eruptive loops of the FL2 are mainly concentrated in the eastern part of the F. This suggests that before the F eruption, there were many coronal loops overlying its eastern part while there were no such loops surrounding its western part. Such a pre-eruptive coronal environment might relate to the inclined eruption of the F and the passage of its western part through the D4R.

At about the time of the event, two CMEs, “CME1” and “CME2”, were observed by LASCO in less than 1 hr. The corresponding LASCO C2 and C3 observations are shown in Figure 4. The CME1 first appeared in the C2 field-of-view (FOV) at 08:06 UT, and later in the C3 FOV at 08:42 UT as a faint loop front filling the SE quadrant but brightest at the South pole. It had a width larger than 104° and a central position angle (P.A.) of 144° . The CME2 was first seen in C2 at 08:50 UT as a much brighter front, and then by 09:18 UT it developed into a full halo with the brightest part spanning 160° from the SE to NW in C3. The CME2 had a central P.A. of 214° and its eruption direction, determined by the central P. A. and plotted in Figure 3, was consistent with that of the erupting F. The average speeds measured by linear fitting are 1223 km s^{-1} at P.A. 168° for the CME1 and 1660 km s^{-1} at P.A. 206°

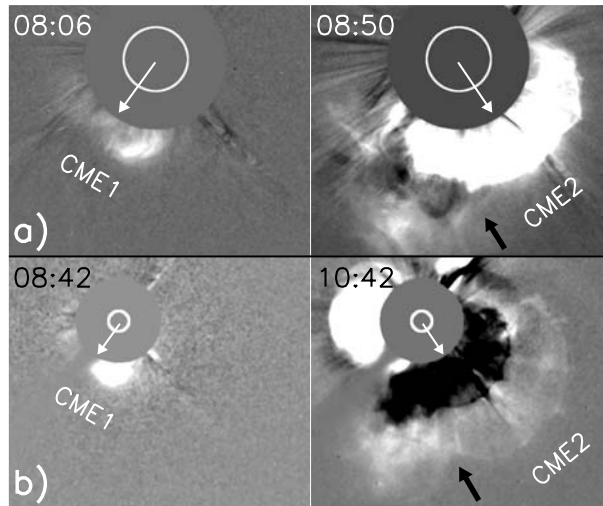


Fig. 4 (a) LASCOC2 and (b) C3 difference images. The white arrows indicate the eruptive directions of the two CMEs, and the black arrows the intersection between their bright fronts.

for the CME2, thus CME2 was faster than CME1. Since the two CMEs were close not only in time but also in space, CME2 tended to overtake CME1. In Figure 4, an overlap of the two CMEs was seen at 08:50 UT when the CME2 came into the C2 FOV, and later can be discerned by 10:42 UT in the C3 FOV (indicated by the black arrows). Similar examples of multiple overlapping CMEs have also been shown by some authors (Simnett & Hudson 1997; Gopalswamy et al. 2002; Moon et al. 2003; Jiang et al. 2008). By applying second-order polynomial fitting, back extrapolation of the CME1 (CME2) front from the height-time (H-T) plots to the eruptive location yields an estimate of the onset time of the CME1 (CME2) near 07:21 UT (08:07 UT). This is very close to the FL1 (FL2) start time at 07:23 (08:12) UT, so the initiations of the two CMEs were probably related to the two flares, respectively. Therefore, the sympathy of the flares indicates that the successive CMEs consisted of a sympathetic pair. We believe that this is the first clear example where sympathetic flares can be associated with the sympathetic occurrence of CMEs, and it is clear that the jet/F interaction provided a critical link between them.

In Figure 5, the projected F height measured from the middle point of the pre-flare F to the top of the erupting F along the CME2 eruption direction on the basis of the $H\alpha$ blue-wing images, the *GOES* soft X-ray flux, the light curves of EIT 195 Å intensities of three dimmings (D1, D3 and D4) and $H\alpha$ intensities of an area near the D4R are plotted, respectively. The extrapolated CME onset times and the average speeds of the CME fronts are also indicated. It is clear that the F began to rise at about the jet start (07:40 UT), strongly implying the interaction and physical connection between them. By the time that F and D4R met (08:08 UT), the F height increased about 6.9×10^4 km and the average speed is estimated to be 41 km s^{-1} during this period. We also see that the two $H\alpha$ brightenings near the D4R occurred just after the first jet appearance and the F meeting with the D4R, suggesting that the western footpoints of the loops were successively disturbed or hit by the jet and the F, respectively. The 195 Å intensities in the D1 showed obvious decreases after the onset of the F eruption, while in the D3 and D4, the obvious decreases were slightly earlier than those in the D1. These 195 Å intensity decreases then continued and persisted through the extrapolated CME2 onset time, indicating further eruptions of the F and the loops, as well as their close relationship with the CME2.

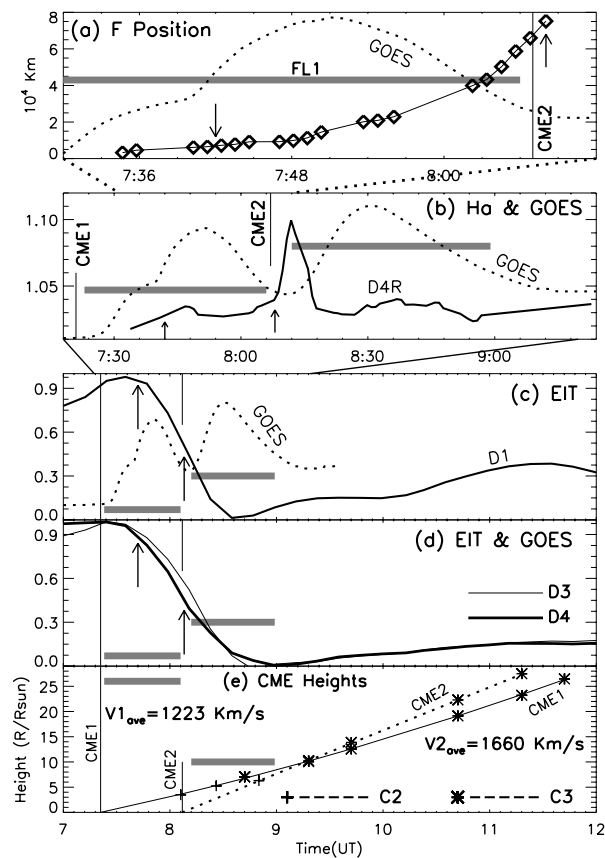


Fig. 5 (a) The projected F height as a function of time (the solid line). Time profiles of *GOES-10* 1–8 Å soft X-ray (the dotted lines), which are displayed in an arbitrary unit to fit in the panels. The light curves of H α line-center intensities (the solid line in (b)) in an area of the D4R (indicated by the box in panel d2 of Fig. 2), and EIT 195 Å intensities (the solid lines in (c) and (d)) in boxes centered on the D1, D3 and D4 (indicated by the boxes in panel e2 of Fig. 1). The value of 1.0 in the H α light curves indicates the mean H α intensity outside the AR before the flares, and the 195 Å light curves are computed from the intensity integrated and normalized over these regions. (e) Heights of the fronts of the two CMEs as a function of time, and the back extrapolations by the use of second-order polynomial fitting. The horizontal bars indicate the durations of the two flares, the vertical bars indicate the extrapolated onset times of the two CMEs, and the two arrows indicate the times of the jet start and the meeting of the F with the D4R, respectively.

4 SUMMARY AND DISCUSSION

In the complex event that was involved in both the sympathetic flare and CME pairs, we can identify three kinds of magnetic interactions: the jet with the F, the jet and the erupting F with the loops. The jet/F interaction took place in a rather straightforward way. The jet spurting out from the FL1 and directly impacted the F. This simultaneously led to the F eruption and the loop disturbances, and so to the D1–D4 formations. Since FL2 resulted from the F eruption, such interaction represented the physical linkage between the two flares. On the other hand, it appears that the loop disappearances were due to the joint effect of the jet/loop and F/loop interactions, which were evidenced by the appearance of the two brightenings after the jet impacted the loops and the erupting F came into contact with the D4R,

respectively. The F/loop interaction led to the progressive developments of the loop disturbances and the D1-D4, and the brief holdup and the only partial passage of the F at the meeting site provided a further remarkable manifestation of such interaction. It is clear that the inclined path of the erupting filament and another magnetic structure barring the eruption are two necessary conditions for the occurrence of a similar interaction (Jiang et al. 2007d). In this case, the loops were located outside the F before the flares but just in the way of its eruption.

Despite the very high spatial and temporal closeness, the two flares, as well as the two CMEs, can be well separated from each other. Since the two CMEs were closely associated with the two flares, respectively, the sympathy of the CMEs was determined by that of the flares. Therefore, the event provides a clear example that the sympathetic CMEs can be related to the sympathetic flares, in which the jet/F interaction play a crucial role in coordinating these eruptive phenomena as an integral process and connecting them as sympathetic pairs. As a matter of fact, some observations have shown that X-ray ejecta or propagation of a surge from an initial eruption region can trigger a sympathetic flare in an adjoining active region (Gopalswamy et al. 1999; Wang et al. 2001). It is also evident that the dense, cool chromospheric mass driven into the filament channel by plasma flow or surge/jet activity from below is important in filament formation and maintenance (Chae et al. 1999a; Wang 1999; Liu et al. 2005). In particular, Liu et al. (2005) showed that some surges can move toward and act on a preexisting nearby filament, and cause its oscillations. In this case, the jet directly hit the F which could exert a destabilizing influence on F. Mass and energy (kinetic and thermal) from the jet were most likely injected into the F since the jet originated from one F end and nearly moved along the F axis. Note that the jet was bright in both EUV and $H\alpha$, so it probably had significantly higher density or temperature than the dark F. Thus, similar to the process described by Wang et al. (2007), the jet injections could cause the heating of the F, which was indicated by its ambiguity in the $H\alpha$ center images, and further acted as a thermal nonequilibrium that triggered the F eruption with the second flare. If so, as noticed by Wang et al. (2001), the erupting F and the CME2 included mass transfer from the site of the FL1 via the jet injections.

An important aspect of the event is the disappearance of the loops due to the jet/loop and F/loop interactions. It is thus possible that both of the CMEs also included contributions from the disappeared loops. Unlike the cases studied by Khan & Hudson (2000) and Jiang et al. (2008), however, the complexity of the event made it difficult to exactly determine which parts of the two CMEs came from the disappeared loops, and we can only infer that the disappeared loops probably simultaneously had a high association with them. Consistent with the jet/loop interaction recently observed by Jiang et al. (2008) and the suggestion that remote brightenings and dimmings resulted from the interaction between an erupting flux rope with overlying loops (Manoharan et al. 1996; Liu et al. 2006; Jiang et al. 2006b), the two appearances of the $H\alpha$ brightenings near the D4R indicated that the jet/loop and F/loop interactions probably involved reconnections between the magnetic fields of loops and of the jet and the erupting F. We believe that the origin and nature of the remote dimmings are the same as the D3-D4 near the two ends of the disappeared loops. The difference is that the loops in this case were clearly seen close to rather than distant from the flares, and they were located outside instead of overlaying the filament channel. Another important aspect of the event is the formation of three sorts of dimmings with different origins. First, the loop-like dimmings simply resulted from the loop disappearances (Khan & Hudson 2000; Jiang et al. 2008). Secondly, the D1 and D2 were related to the F eruption and composed BDDs (Sterling & Hudson 1997; Jiang et al. 2006a; Jiang et al. 2007c). Thirdly, the D3 and D4 were due to the loop disappearances. Similar to the BDDs, they probably represented the evacuated feet of the disappeared loops (Jiang et al. 2008), so they can be regarded as another kind of BDDs. Therefore, two pairs of BDDs, D1-D2 and D3-D4, were formed during this event. They were located in the opposite-polarity regions near the four ends of the two magnetic systems that can interact with each other, and it appears that the mass loss originating from them could also provide mass to supply the CMEs. Here, we introduce a new term and call them “quadrupolar dimmings”, and it will be interesting to examine whether quadrupolar dimmings also occur in the cases of remote dimmings.

Acknowledgements We thank an anonymous referee for many valuable comments and constructive suggestions, which improved the quality of this paper. We thank the *TRACE* team, the *SOHO*/MDI, EIT

and LASCO teams for our free access to data. We are grateful to the observing staff at YNAO and KSO for making good observations. This work is supported by the 973 Program (2006CB806303), by the Scientific Application Foundation of Yunnan Province under grant 2007A112M, and by the National Natural Science Foundation of China (NSFC) under grants 10573033 and 40636031.

References

- Aschwanden, M. J. 2004, *Physics of the Solar Corona-an Introduction* (New York: Springer)
- Brueckner, G. E., et al. 1995, *Sol. Phys.*, 162, 357
- Chae, J., Denker, C., Spirock, T. J., et al. 1999a, *Sol. Phys.*, 195, 333
- Chae, J., Qiu, J., Wang, H., et al. 1999b, *ApJ*, 513, L75
- Cheng, J., Fang, C., Chen, P., et al. 2005, *ChJAA (Chin. J. Astron. Astrophys.)*, 5, 265
- Delaboudinière, J. -P., et al. 1995, *Sol. Phys.*, 162, 291
- Handy, B. N., et al. 1999, *Sol. Phys.*, 187, 229
- Goff, C. P., van Driel-Gesztelyi, L., Démoulin, P., et al. 2007, *Sol. Phys.*, 240, 283
- Gopalswamy, N., Nitta, N., Manoharan, P. K., et al. 1999, *A&A*, 347, 684
- Gopalswamy, N., Yashiro, S., Michalek, G., et al. 2002, *ApJ*, 572, 103
- Kahler, S. W., Moore, R. L., Kane, S. R., & Zirin, H. 1988, *ApJ*, 328, 824
- Khan, J. I., & Hudson, H. S. 2000, *Geophys. Res. Lett.*, 27, 1083
- Jiang, Y., Li, L., & Yang, L. 2006a, *ChJAA (Chin. J. Astron. Astrophys.)*, 6, 345
- Jiang, Y., Li, L., Zhao, S., et al. 2006b, *New Astron.*, 11, 612
- Jiang, Y., Chen, H., Li, K., et al. 2007a, *A&A*, 469, 331
- Jiang, Y., Shen, Y., & Wang, J. 2007b, *ChJAA (Chin. J. Astron. Astrophys.)*, 7, 129
- Jiang, Y., Yang, L., Li, K., et al. 2007c, *ApJ*, 662, L131
- Jiang, Y., Yang, L., Li, K., et al. 2007d, *ApJ*, 667, L105
- Jiang, Y., Shen, Y., Bi, Y., et al. 2008, *ApJ*, 677, 699
- Liu, Y., Kurokawa, H., & Shibata, K. 2005, *ApJ*, 631, L93
- Liu, C., Lee, J., Deng, N., et al. 2006, *ApJ*, 642, 1205
- Manoharan, P. K., van Driel-Gesztelyi, L., Pick, M., et al. 1996, *ApJ*, 468, L73
- Miklenic, C. H., Veronig, A. M., Vršnak, B., et al. 2007, *A&A*, 461, 697
- Moon, Y.-J., Choe, G. S., Park, Y. D., et al. 2002, *ApJ*, 574, 434
- Moon, Y.-J., Choe, G. S., Wang, H., et al. 2003, *ApJ*, 588, 1176
- Otruba, W., & Pötzi, W. 2003, *Hvar Obs. Bull.* 27, 189
- Pearce, G., & Harrison, R. A. 1990, *A&A*, 228, 513
- Scherrer, P. H., et al. 1995, *Sol. Phys.*, 162, 129
- Shi, Z.-X., Wang, J.-X., & Luan, D. 1997, *Acta Astro. Sinica*, 38, 257
- Simnett, G. M., & Hudson, H. 1997, in *Proc. 31st ESLAB Symp., Correlated Phenomena at the Sun, in the Heliosphere and in Geospace*, ed. A. Wilson (ESA-SP-415: Noordwijk), 437
- Sterling, A. C., & Hudson, H. S. 1997, *ApJ*, 491, L55
- Švestka, Z., Farnik, F., & Tang, F. 1990, *Sol. Phys.*, 127, 149
- Thompson, B. J., Plunkett, S. P., Gurman, J. B., et al. 1998, *Geophys. Res. Lett.*, 25, 2465
- Wang, H., Chae, J., Yurchyshyn, V., et al. 2001, *ApJ*, 559, 1171
- Wang, H., Liu, C., Jing, J., et al. 2007, *ApJ*, 671, 973
- Wang, Y.-M. 1999, *ApJ*, 520, L71
- Wheatland, M. S., & Craig, I. J. D. 2006, *Sol. Phys.*, 238, 73
- Zhang, C., Wang, H., Wang, J., et al. 2000, *Sol. Phys.*, 195, 135